Microclimatic behavior of a screen house proposed for horticultural production in low-altitude tropical climate conditions

Edwin Villagran[1]* , Jorge Eliecer Jaramillo[2]

[1]Corporación Colombiana de Investigación Agropecuaria - Centro de Investigación Tibaitata, Mosquera, Colombia
[2]Corporación Colombiana de Investigación Agropecuaria - Centro de Investigación La Selva, Rionegro, Colombia
*Corresponding author, e-mail: eavillagranm@unal.edu.co

Abstract

In developing countries, horticultural production in low-altitude tropical climate conditions is often limited by biotic and abiotic factors. In these countries, the implementation of highly technical greenhouses is not feasible due to economic, social and cultural issues related to farmers. Therefore, one of the alternatives that has taken a great boom is the use of screen house structures (SH), although information on the microclimatic behavior of these is still limited. The objective of this research was to use an experimentally validated 3D CFD numerical simulation model to study the thermal behavior and airflow patterns in an SH located in the Colombian Caribbean region during the daytime hours (6:00 to18:00 h). The results obtained showed that the air flow patterns inside the SH showed speed reductions of up to 68% with respect to the speed of the external wind. It was also found that the thermal behavior inside the SH was quite homogeneous, the average temperature values in the structures ranged between 23.9 and 39 °C and the difference with external environment temperature did not exceed 1.8 °C. It was concluded that the implementation of this type of structure could be an useful technological tool for the optimization of horticultural production in low-altitude tropical climate regions.

Keywords: airflow, CFD simulation, family farming, food security, thermal behavior

Introduction

The annual national production in Colombia of fruits and vegetables (F&V) is approximately 9.22 million tons of which 7.75 are fruits and 1.43 are vegetables. The horticultural sector contributes in approximately 6% to the national production of vegetables and is strongly concentrated in the Andean region, while in the Caribbean region it is not a relevant agricultural activity and production is carried out in small areas mainly in a family farming contexts (Martínez-Reina et al., 2019; Rodríguez-Leyton, 2019). The main factors that limit horticultural production in the Colombian Caribbean are related to climatic factors. In this region, high radiation and temperature conditions predominate, which will be increasingly intense due to climate change. On the other hand, the open field production approach that currently exists in this region, and in many warm tropical regions, increases the vulnerability of crops to pests and diseases

and to adverse ecophysiological conditions such as water stress, the salinity and high temperature of the soil (Pérez Vega et al., 2016; Priya et al., 2019; Akrami & Arzani, 2019).

In developing countries one of the technically and economically viable alternatives for the sustainable intensification of agricultural production in low-altitude tropical climate is the use of screen-houses (SH) structures. SH is widely used in warm and arid Mediterranean climates (Al-Mulla et al., 2008), this technological adaptation of the productive system allows the construction of an enclosure where the cover and the lateral walls are made of insect screens to limit the entry of some pests, to mitigate the negative effect of severe climates, to reduce the water consumption of the plants, to change the spectrum of the solar radiation and the related physiological benefits, as well as to reduce pesticides applications of, and improve the yield and final quality of the crops (Guo et al., 2015;

Vidogbéna et al., 2015; Teitel et al., 2017; Mahmood et al., 2018; Mupambi et al., 2018; Yang et al., 2018; Alvarado et al., 2020).

The SH generally are a simpler and less expensive structure than the greenhouses, these are constructed on pillars of metal or wood and on a cover support made in steel cables, in the lateral walls are installed insect screens and in the cover are installed shade cloths or insect screens (Mahmood et al., 2018). The use of these insect screens causes alterations to the microclimate generated inside the SH mainly due to a modification of the air movement regime and a reduction in air speed which could cause a decrease in CO_2 levels, increases in humidity and temperature that can influence plant physiological processes such as photosynthesis and transpiration rates with negative effects on crop growth and development (Bournet & Boulard, 2010). Although it should be noted that these microclimate alterations are generally less drastic in greenhouses with plastic cover and with a good management of the screens is possible to reduce the indoor temperature(Pirkner et al., 2014; Perillo et al., 2015; Liu et al., 2017; Xu et al., 2017).

The study of the microclimatic behavior of SH is not as generalized as that of conventional greenhouses, but probably has contributed empirically to the implementation of SH despite the lack of research on aspects such as architecture, the geometry of the structure and the type of mesh used (Flores-Velazquez et al., 2017). The existing studies on the microclimate in the SH have been addressed mainly through experimental approaches and through numerical computational fluid simulation (CFD) as can be reviewed in Mahmood et al. (2018), and in studies analyzing thermal and aerodynamic behavior (Tanny et al., 2008; Teitel et al., 2014, 2017), as well as the effect of the screen pore size (Kalcsits et al.,

2017; Tanny et al., 2018), and the shape and geometry of the structure (Flores-Velazquez et al., 2013).

The objectives of this study were to validate experimentally a 3D CFD numerical simulation model under the dominant climatic conditions of the Colombian Caribbean and, using the validated model, to study the daytime behavior of the airflow patterns and thermal behavior of an asymmetrically roofed screen-house structure built in the experimental area.

Materials and Methods
Description of the screen-house

The development of this research was carried out in a SH with an asymmetric roof and a covered floor area of 740 m² located in the Colombian Caribbean region in the municipality of Seville, department of Magdalena, at the Caribbean Research Center of the Colombian Corporation for Agricultural Research – AGROSAVIA (longitude: 74°10´ W, latitude: 10°47´ W and altitude: 18 m.a.s.l). The cross axis of the structure was located in an east-west direction (E-W). The SH had a cross section (x-axis) and longitudinal section (z-axis) of 37 and 20 m in dimension, respectively, the SH had a minimum height of 2.5 m on the sides and a maximum height of 6.7 in the central zone (Figure 1). The side walls and roof were covered with a semi-transparent insect proof screen with a thread count of 16.1 x 10.1 for each cm⁻² and a porosity (ε) of 0.33.

The region under study presents some climatic conditions where the average multiannual average temperature for a period of 30 years is 29.2 °C, with an average maximum and minimum of 36.8 and 23.2 °C, respectively, the relative humidity presents an average behavior with values above 60%, the annual precipitation some average values of 1245. 1 mm.
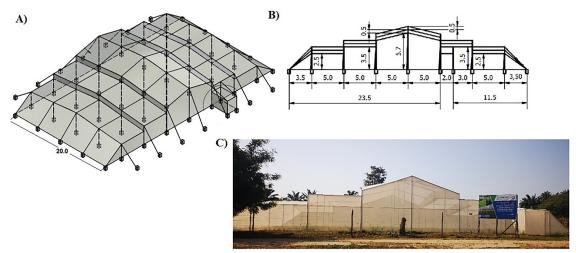

Figure 1. A) General scheme of the screen-house, B) Dimensions of the structure and, C) Image of the real prototype.

Collection of experimental data

For the development of the simulations a scheme was established to record data both inside and outside the SH, during the period between November 1st, 2019 and January 31st, 2020, data were recorded with a logging interval of 10 minutes. In the outside environment the climatic variables temperature, air humidity, wind speed and direction, solar radiation, were recorded with a Davis-Vantage 2 plus 6162 weather station (Davis Instruments, Hayward, CA, USA). Inside the SH at 1.5 m above ground level (y-axis), five micro weather stations (WatchDog 1000, Spectrum Technologies, Aurora, IL), were used to record and store the air temperature values of the SH (Figure 2). This evaluation period is valid for the application of the CFD model and for the objective of the study since the climatic conditions in the intertropical region do not present great variations on a monthly scale, as is the case in other regions where the four seasons are present.
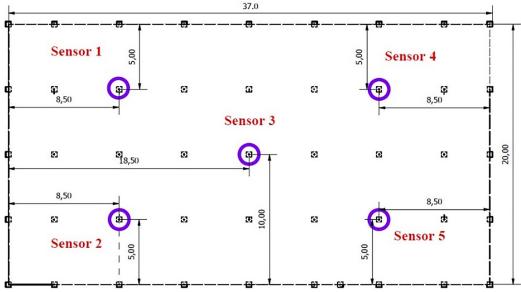

Figure 2. Experimental scheme for recording and capturing temperature data inside the screen-house.

CFD model

Numerical CFD models allow the development of a technique to solve a set of non-linear partial differential equations through numerical resolution methods by which these equations are discretized to a system of linear equations. The CFD methodology allows calculating the air flow patterns and the thermal distribution patterns generated inside a SH, the transport phenomena via free convection can be described by the following general transport equation for a fluid in steady state:

$$\frac{\partial(u_\phi)}{\partial x} + \frac{\partial(v_\phi)}{\partial y} + \frac{\partial(w_\phi)}{\partial z} = \Gamma\nabla^2\phi + S_\phi \quad (1)$$

Where y, x and z represent the coordinates in Cartesian space, u, v and w are the components of the velocity vector, ∇^2 is the Laplacian operator, Γ is the diffusion coefficient, ϕ represents the concentration of the transported quantity in a dimensional shape (moment, mass and energy), y S_ϕ is the source term.

The airflow modeled considered the turbulence through the standard k - ε model, this is a semi-empirical model based on the transport equations that solve k kinetic turbulent energy and the dispersion of this energy per unit volume ε, the k - ε has been the most applied and widely validated model in greenhouse or SH airflow studies showing to be efficient with the use of computational resources and providing realistic solutions (Villagrán et al., 2019). The Boussinesq model was considered to simulate and calculate the variations in air density inside the SH generated by temperature changes. The lateral and frontal surfaces and SH cover were modelled using equations derived from the flow of a free and forced fluid through porous materials, taking into account their main characteristics of porosity and permeability (Valera et al., 2005). These equations can be derived from the Forchheimer equation:

$$\frac{\partial p}{\partial x} = \frac{\mu}{K}u + \rho\frac{Cf}{\sqrt{K}}u|u| \qquad (2)$$

Where u is the air speed (m s^{-1}); μ is the dynamic viscosity of the fluid (kg m^{-1} s^{-1}), K is the permeability of the medium (m²); cf is the inertial factor of the screen; ρ is the density of the air (kg m^{-3}), y ∂x the thickness of the porous material (m). The effect of solar radiation was included in the numerical model by establishing a heat flux on the ground surface of the SH as a function

of the incident solar radiation and the transmission of the roofing material (Villagrán & Bojacá, 2019b). Also, in order to simplify the resolution of the 3D CFD model, no crops were included, this in order to speed up the numerical calculation and establish the behavior of the air flow and temperature under the worst possible scenario, i.e. under conditions where no plants are present.

Meshing and boundary conditions

For the development of the simulations, a large computer domain was created and included the SH and its surroundings (Figure 3A and 3 B). The dimensions of the computational domain in each of the axes (x-y-z) were established according to the recommendations established for CFD simulation (Perén et al., 2016).
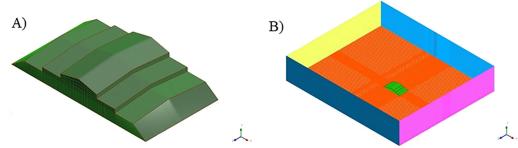

Figure 3. A) Detail of the meshing of the screen-house and B) Detail of the computer domain.

In the process of mesh generation, an unstructured grid of square elements was selected with a total of 18.171.713 elements. The density of the mesh was increased in the regions near the screens, floor, side and roof areas which are the regions where relevant thermal gradients are usually found and which in turn were simulated with the improved wall treatment. The independence of the solutions to the size of the mesh, as well as the quality of the mesh was carried out following the procedure established by He et al. (2017)

and successfully implemented by Villagrán et al. (2019). The quality of the mesh was established by means of the 3 X 3 relative determinant calculation, which showed a behavior higher than 92.2 % with cells between 0.95 and 1 which indicates elements of perfectly regular mesh (Ansys, 2017). In each of the numerical simulations, the specific boundary conditions for each part of the domain and the physical properties of the materials in the computer domain and the SH (Table 1).

Table 1. Main parameters of the CFD simulation model.

Simulation hypotheses	
Simulation type	3D-Steady state second order, solver pressure segregated
Viscosity model	Standard k - ε
Energy Equation	Activated with improved wall treatment and buoyancy effects.
Radiation model	Deactivated, Surface heat flow is imposed.
Porous medium	Porous screen 16.1x10.2 y porosity ε = 0.33.
Boundary conditions	
Domain entry	Logarithmic speed profile via UDF. $v(y) = \dfrac{v^*}{K} \, ln \left(\dfrac{y + y_0}{y_0} \right)$
Domain exit	Pressure output condition.
Roof of the domain	Symmetrical conditions.
Treatment of porous media	Viscous effect due to the netting (a)=3.98 e^{-9} and drag coefficient (C_2) 19185
Roof and walls of the screenhouse	Porous media treatments
Convergence criteria	10^{-6} for the energy equation and 10^{-3} for the equations of momentum, continuity and turbulence.
Physical properties of materials	

	Air	Soil	Porous Screen
Density (ρ, kg m^{-3})	1.225	1300	990
Thermal conductivity (k, W m^{-1} K^{-1})	0.0242	1.6	0.33
Specific heat (Cp, J K^{-1} kg^{-1})	1006.43	1738	1900
Coefficient of thermal expansion (K^{-1})	0.0033		

Calibration of the CFD model and simulated cases

The calibration and adjustment of the CFD model was done by comparing the average data obtained in each of the sensors (1-5) installed inside SH and the data obtained by CFD simulation in each of the positions of the five sensors. This was done through a goodness-of-fit analysis with criteria such as mean absolute error (MAE) and mean square error (RMSE).

$$MAE = \frac{1}{m}\sum_{i=1}^{m}|Tmi - Tsi| \qquad (3)$$

$$RMSE = \sqrt{\frac{\sum_{i=1}^{m}|Tmi-Tsi|^2)}{m}} \qquad (4)$$

Where Tmi and Tsi are the value of the experimental temperature and the value of the simulated temperature respectively and m the number of data compared, it was also plotted the trend of the simulated and experimental data sets.

Once the fit of the CFD model was verified, it was used to determine the thermal behavior and airflow patterns within the SH, each simulation included specific initial conditions recorded in the SH external environment for the hours of the day between 6:00 and 18:00 (Table 2).

Table 2. Initial conditions for each simulation established in the external SH environment.

Hour	Temperature (°C)	Solar radiation (w m^{-2})	Wind speed (m s^{-1})	Wind direction
6	23.6	25.67	0.78	ENE
7	25.8	52.44	1.04	ENE
8	29.1	119.8	1.10	ENE
9	32.4	287.1	1.23	E
10	34.8	540.4	1.65	E
11	36.6	703.1	1.78	ESE
12	37.4	803.6	1.91	E
13	38.0	860.8	1.93	WSW
14	37.6	818.4	1.56	WSW
15	36.5	688.5	1.45	W
16	35.1	409.5	1.32	W
17	33.1	204.1	1.15	WNW
18	30.1	142.3	0.93	WNW

Results and Discussion
CFD model calibration

The qualitative behavior of the simulated and measured temperature values at the individual measuring sensor positions showed a similar trend on the evaluated time scale (Figure 4). On the other hand, in quantitative terms, the MAE values obtained were 0.42, 0.36, 0.30, 0.22 and 0.23 °C, while the RMSE values were 0.52, 0.44, 0.36, 0.27 and 0.29 °C for sensors 1 to 5, respectively. According to these results it can be mentioned that the numerical model is able to predict in an adequate way the thermal behavior of SH, so its use for the objectives of this research was accurate.
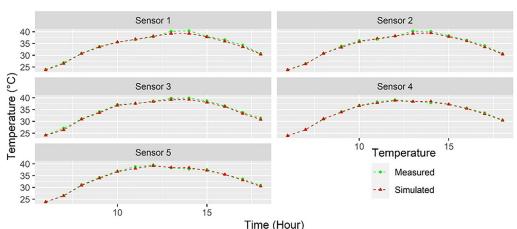

Figure 4. Measured and simulated temperature behavior (°C) between 6:00 and 18:00 hours.

The simulated airflow patterns showed a behavior in which a fraction of the airflow approaching the windward side of the SH (x-axis) rises towards the roof area of the structure, part of this airflow collides with the first side of the asymmetrical roof and creates an airflow that is directed from this part of the SH roof towards the crop area and then out of the SH on the leeward side (Figure 5), this behavior is similar at 7, 13 and 17 hours of the day and differs from that reported by Teitel & Wenger (2012) in a numerical study conducted for flat-roof SH,

where a large part of the airflow leaves the structure through the roof area; therefore we can conclude that the difference in flow pattern may be influenced by the shape of the SH roof evaluated in this study, which due to its shape causes pressure gradients that allow airflow into

the SH (Flores-Velazquez et al., 2013). On the other hand, another common feature in the airflow patterns for this structure is a convective cell that forms over the central zone of the SH (z-axis), where the airflow vectors move from the floor area to the roof of the structure (Figure 5).
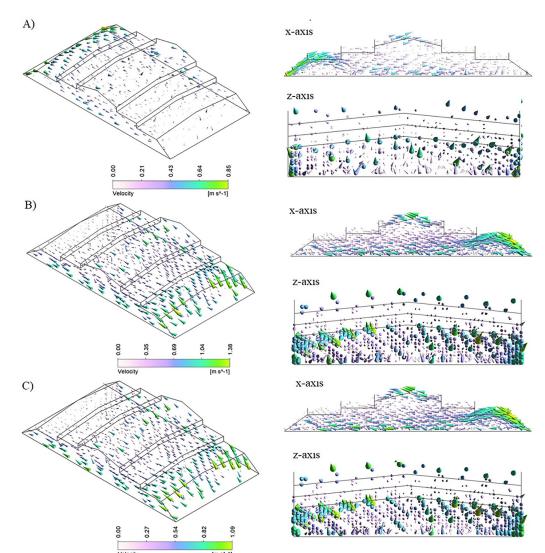

Figure 5. Simulated airflow distribution patterns (m s^{-1}) in plan isometric view, front view and side view for, A) Hour 7, B) Hour 13 and C) Hour 17

Also qualitatively a pattern of air movement can be observed inside the SH where the air flows that move near the front walls of the structure, which are parallel to the flow of external air are presented vectors of greater speed, this is because in this type of structure where the cover is a porous material promotes the exchange of air between the external and internal environment near these regions, therefore they are areas that have a higher degree of ventilation (Flores-Velazquez et al., 2017; Teitel et al., 2015).

In quantitative terms, the average airflow velocity for each simulated hour ranges from 0.25 to 0.76 m s^{-1} (Table 3). The normalized speed, which represents the ratio of the indoor airflow speed to the outdoor
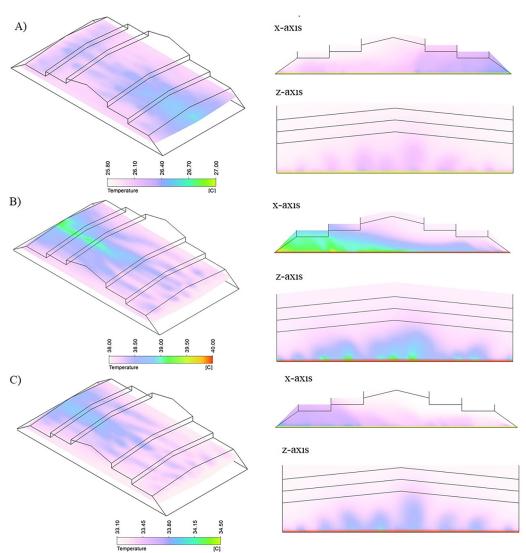
airflow speed, showed a significant reduction in the air movement speed inside the SH with values up to 68% lower than the outdoor wind speed value (Table 3), this is due to the fact that the porous screens modify the speed and turbulence characteristics of the flow pattern and the presence of this type of screen exerts a friction effect and a drag coefficient that opposes the flow of air outside and generates a loss of air flow speed inside as a function of the porosity of the screen used (Teitel et al., 2020). The values found for this study are within the range reported in a previous study by Flores-Velazquez et al. (2013) and are slightly higher than those calculated for Teitel et al. (2018).

Table 3. Airflow pattern parameters obtained by CFD simulation.

Hour	Average velocity (ms⁻¹)	Normalized velocity
6	0.25	0.32
7	0.35	0.33
8	0.37	0.34
9	0.43	0.35
10	0.59	0.36
11	0.64	0.36
12	0.75	0.39
13	0.76	0.39
14	0.53	0.34
15	0.54	0.37
16	0.46	0.35
17	0.56	0.36
18	0.41	0.34

Thermal behavior

One of the factors that generates most interest and concern for study in protected agriculture is the spatial distribution of temperature inside structures, since the behavior of this variable is a factor that affects the growth and development of plants. The simulated thermal distribution in the x and z axes, as well as in a plan view at a height of 1.5 m above ground level, allowed us to observe that inside the SH there is a heterogeneous temperature behavior, where the cooler regions are located on the windward side and the warmer regions are located on the central and leeward side of the SH (Figure 6). This thermal distribution behavior is related to the air flow fields, therefore, higher speed regions are the cooler temperature regions and on the contrary the warm regions are presented in the areas of lower flow velocity, this is characteristic of the ventilation phenomenon in screen houses (Al-Mulla et al., 2008; Flores-Velazquez et al., 2013) and greenhouses (Villagrán & Bojacá, 2019a).

Figure 6. Simulated spatial temperature distribution (°C) in plan isometric view, front view and side view for, A) Hour 7, B) Hour 13 and C) Hour 17.

The analysis of the thermal behavior was complemented with the calculation of average temperatures inside the SH (T_{in-SH}) for each hour between 6 and 18 h, the thermal differential between the inside and outside environment (Δ_T) and finally the thermal differentials (D_T) between the warmest and coolest zone on each of the axes (x, y, z) indoors of SH (Table 4). The values de T_{in-SH} this process of heating the volume of air inside the SH as the hours pass from morning to noon, is a heating generated jointly by the increase in external environment temperature and external solar radiation, as well as the subsequent process of cooling that occurs from 14 to 18 h (Table 4).

Table 4. Thermal parameters obtained by CFD simulation.

Hour	T_{in-SH}(°C)	Δ_T(°C)	$D_T x$(°C)	$D_T z$(°C)	$D_T y$(°C)
6	23.9	0.30	0.3	0.2	0.3
7	26.4	0.62	0.4	0.6	0.9
8	30.8	1.78	0.6	0.7	1.1
9	33.6	1.28	0.6	0.8	1.3
10	36.3	1.50	1.1	1.3	1.5
11	37.5	0.90	1.4	1.3	1.7
12	38.5	1.14	1.7	1.5	1.5
13	38.9	0.90	1.8	1.2	1.5
14	39.0	1.40	1.2	1.3	1.4
15	37.6	1.14	0.9	1.0	1.0
16	35.8	0.74	0.8	0.9	0.8
17	33.3	0.24	0.6	0.8	0.6
18	30.4	0.40	0.3	0.4	0.5

On the other hand, the values of Δ_T obtained were within the range of 0.3 and 1.5 °C, these thermal differentials between outdoor and indoor environment are generated due to an energy accumulation that occurs in the interior of SH and that natural ventilation is not able to remove, it should be noted that these values of ΔT were obtained in a non-cultivation scenario, therefore it can be expected that the Δ_T under crop conditions are lower due to the contribution of heat transfer and mass that plants generate, therefore the temperature in the interior of SH is similar to the temperature or even lower as demonstrated by Xu et al. (2017). The temperature homogeneity in each of the axes studied showed minimum variations between the coolest point and the hottest point, D_T of 0.3, 0.2 and 0.3 °C for x, z and y, respectively, while the maximum values were 1.8, 1.3 and 1.7 °C for the same axes (Table 4). The mean values of D_T for the simulated 13 hours were 0.9, 0.92 and 1.2 °C in x, z and y, these values can be considered adequate and are below the maximum range recommended for protected agriculture (±2 °C) (Zorzeto et al., 2014).

Based on these results, it can be concluded that the use of screen house structures is a technological and sustainable option for protected agriculture that is applicable to warm regions in developing countries, where one of the objectives of small horticultural producers is to optimize the resources used for food production and increase crop yields and product quality as a strategy to ensure food security in these communities. Under these temperature conditions it is possible to establish horticultural species such as; tomato, cucumber, pepper and eggplant, species for which at a commercial level there are planting materials with some characteristics that allow them to have a better adaptation to these high temperature conditions and provide acceptable final yields. This technology can also be an option to boost the consumption of F&V in children populations and thus solve the public health problem generated by nutritional deficiencies caused by diets based mainly on cereals, since F&V provide a series of vitamins, minerals and nutraceuticals properties that are essential to the healthy diet of human beings (Alzate T et al., 2017; Aune et al., 2017; Tak et al., 2019; Kähkönen et al., 2020).

Future work for these types of climatic conditions should focus on developing agronomic and physiological studies, such as assessments of crop response to different planting densities, different management practices, irrigation and fertilization management, quantification of growth and development, variety evaluation. This will allow the establishment of production models under cover of different horticultural crops of interest, seeking to increase the technological tools available for agricultural production for these small farms that operate under the model of family farming and that undoubtedly are and will be of great importance to achieve the goals of the Sustainable Development Objectives and mainly contribute to ensuring food resources that by 2050 should be for a population of approximately 9 billion (Ortiz et al., 2018; Wuepper et al., 2020).

Conclusions

The implementation of a screen house structure is suitable for the optimization of horticultural production of small producers in low-altitude tropical climate regions. The air flow patterns inside the structure were affected by the presence of the porous screen which generated reductions in the speed of the air flow inside with respect to the air flow in the outside environment, although the average speeds obtained in the SH were 0.25 and 0.76 ms^{-1} and are in the range of the recommended value for crops established under protected agricultural structures. The spatial temperature behavior of this type of structure is homogeneous and the value of this variable does not differ by more than 1.7 °C with respect to the external environment temperature. Therefore, screen houses can

be a technological tool to mitigate the vulnerability of crops to extreme weather conditions as well as to pests and diseases, contributing directly to the sustainability of family farming and the food security of the population.

References

Al-Mulla, Y.A., Al-Balushi, M., Al-Rawahy, M., Al-Raisy, F., Al-Makhmary, S. 2008. Screenhouse microclimate effects on cucumber production planted in soilless culture (open system). *Acta Horticulturae* 801: 637-644.

Alvarado, K.A., Mill, A., Pearce, J.M., Vocaet, A., Denkenberger, D. 2020. Scaling of greenhouse crop production in low sunlight scenarios. *Science of The Total Environment* 707: 136012.

Alzate T, L.M., González, D., Hincapié, S., Londoño-Londoño, J., Jiménez-Cartagena, C. 2017. The profile of bioactive substances in ten vegetable and fruit by-products from a food supply chain in Colombia. *Sustainable Production and Consumption* 9: 37-43.

Ansys. ANSYS Fluent Tutorial Guide. 2017. http://users.abo.fi/rzevenho/ansys%20fluent%2018%20tutorial%20guide.pdf <Access on 10 Nov. 2019>

Akrami, M., Arzani, A., 2019. Inheritance of fruit yield and quality in melon (*Cucumis melo L.*) grown under field salinity stress. *Scientific Reports*, 9: 1-13.

Aune, D., Giovannucci, E., Boffetta, P., Fadnes, L.T., Keum, N., Norat, T., Tonstad, S. 2017. Fruit and vegetable intake and the risk of cardiovascular disease, total cancer and all-cause mortality—a systematic review and dose-response meta-analysis of prospective studies. *International journal of epidemiology* 46: 1029-1056.

Bournet, P.E., Boulard, T. 2010. Effect of ventilator configuration on the distributed climate of greenhouses: A review of experimental and CFD studies. *Computers and electronics in agriculture* 74: 195-217.

Flores-Velazquez, J., Guerrero, F.V., Lopez, I.L., Montero, J.I., Piscia, D. 2013. 3-Dimensional thermal analysis of a screenhouse with plane and multispan roof by using computational fluid dynamics (CFD). *Acta Horticulturae* 1008: 151–158.

Flores-Velazquez, J., Ojeda, W., Villarreal-Guerrero, F., Rojano, A. 2017. Effect of crops on natural ventilation in a screenhouse evaluated by CFD simulations. *Acta Horticulturae* 1170: 95–101.

Guo, Z., Liu, H., Yuan, H., Yang, G., Zheng, J., Chen, L. 2015. Insect-proof nets affect paddy field microclimate parameters and grain quality of different japonica rice varieties. *Journal of Crop Science and Biotechnology* 18: 73-81.

He, X., Wang, J., Guo, S., Zhang, J., Wei, B., Sun, J., Shu, S. 2017. Ventilation optimization of solar greenhouse with removable back walls based on CFD. *Computers and Electronics in Agriculture*. 149:16-25.

Kähkönen, K., Hujo, M., Sandell, M., Rönkä, A., Lyytikäinen, A., Nuutinen, O. 2020. Fruit and vegetable consumption among 3–5-year-old Finnish children and their parents: Is there an association?. *Food Quality and Preference* 82: 103886.

Kalcsits, L., Musacchi, S., Layne, D.R., Schmidt, T., Mupambi, G., Serra, S., Khot, L.R. 2017. Above and below-ground environmental changes associated with the use of photoselective protective netting to reduce sunburn in apple. *Agricultural and Forest Meteorology* 237: 9-17.

Liu, X., Xu, G., Wang, Q., Hang, Y. 2017. Effects of insect-proof net cultivation, rice-duck farming, and organic matter return on rice dry matter accumulation and nitrogen utilization. *Frontiers in Plant Science* 8: 1-15.

Mahmood, A., Hu, Y., Tanny, J., Asante, E.A. 2018. Effects of shading and insect-proof screens on crop microclimate and production: A review of recent advances. *Scientia Horticulturae* 241: 241-251.

Martínez-Reina, A.M., Tordecilla-Zumaqué, L., Grandett-Martínez, L.M., Del Valle Rodríguez-Pinto, M., Cordero-Cordero, C.C., Silva-Acosta, G.E., Orozco-Guerrero, A.R. 2019. Análisis económico de la producción de berenjena (*Solanum melongena* L.) en dos zonas productoras del Caribe colombiano: Sabanas de Sucre y Valle del Sinú en Córdoba. *Ciencia y Agricultura* 16: 17-34.

Mupambi, G., Anthony, B.M., Layne, D.R., Musacchi, S., Serra, S., Schmidt, T., Kalcsits, L. A. 2018. The influence of protective netting on tree physiology and fruit quality of apple: A review. *Scientia Horticulturae* 236: 60-72.

Ortiz, W., Vilsmaier, U., Osorio, Á.A. 2018. The diffusion of sustainable family farming practices in Colombia: an emerging sociotechnical niche? *Sustainability Science* 13: 829-847.

Perén, J.I., van Hooff, T., Leite, B.C.C., Blocken, B. 2016. CFD simulation of wind-driven upward cross ventilation and its enhancement in long buildings: Impact of single-span versus double-span leeward sawtooth roof and opening ratio. *Building and Environment* 96: 142-156.

Pérez Vega, C., Ramírez Arias, J.A., López Cruz, I.L. 2016. Características aerodinámicas de mallas anti-insectos usadas en ventanas de invernaderos en México. *Revista Mexico Ciencias Agrícolas* 7: 493–506.

Perillo, A.C., Kucharik, C.J., Meehan, T.D., Serbin, S.P., Singh, A., Townsend, P.A., Gratton, C. 2015. Use of insect exclusion cages in soybean creates an altered microclimate and differential crop response. *Agricultural and Forest Meteorology* 208: 50-61.

Pirkner, M., Tanny, J., Shapira, O., Teitel, M., Cohen, S., Shahak, Y., Israeli, Y. 2014. The effect of screen type on crop micro-climate, reference evapotranspiration and yield of a screenhouse banana plantation. *Scientia Horticulturae* 180: 32-39.

Priya, M., Sharma, L., Kaur, R., Bindumadhava, H., Nair, R.M., Siddique, K.H.M., Nayyar, H. 2019. GABA (γ-aminobutyric acid), as a thermo-protectant, to improve the reproductive function of heat-stressed mungbean plants. *Scientific Reports* 9: 1-14.

Rodríguez-Leyton, M. 2019. Desafíos para el consumo de frutas y verduras. *Revista de la Facultad de Medicina Humana* 19: 105-112.

Tak, M., Shankar, B., Kadiyala, S. 2019. Dietary transition in India: temporal and regional trends, 1993 to 2012. *Food and Nutrition Bulletin* 40: 254-270.

Tanny, J., Lukyanov, V., Neiman, M., Cohen, S., Teitel, M., Seginer, I. 2018. Energy balance and partitioning and vertical profiles of turbulence characteristics during initial growth of a banana plantation in a screenhouse. *Agricultural and Forest Meteorology* 256: 53-60.

Tanny, J., Teitel, M., Barak, M., Esquira, Y., Amir, R. 2008. The effect of height on screenhouse microclimate. *Acta Horticulturae* 801: 107–114.

Teitel, M., Garcia-Teruel, M., Alon, H., Gantz, S., Tanny, J., Esquira, I., Sofer, M., Levi, A., Schwartz, A., Antler, A. 2014. The Effect of Screenhouse Height on Air Temperature. *Acta Horticulturae* 1037: 517–523.

Teitel, M., Garcia-Teruel, M., Ibanez, P.F., Tanny, J., Laufer, S., Levi, A., Antler, A. 2015. Airflow characteristics and patterns in screenhouses covered with fine-mesh screens with either roof or roof and side ventilation. *Biosystems Engineering* 131: 1-14.

Teitel, M., Liang, H., Tanny, J., Garcia-Teruel, M., Levi, A., Ibanez, P. F., Alon, H. 2017. Effect of roof height on microclimate and plant characteristics in an insect-proof screenhouse with impermeable sidewalls. *Biosystems Engineering* 162: 11-19.

Teitel, M., Liang, H., Vitoshkin, H., Tanny, J., Ozer, S. 2020. Airflow patterns and turbulence characteristics above the canopy of a tomato crop in a roof-ventilated insect-proof screenhouse. *Biosystems Engineering* 190: 184-200.

Teitel, M., Rguez, M.G.T., Liang, H., Tanny, J., Ozer, S., Alon, H. 2018. Vertical profiles of temperature, humidity ratio and air velocity in different types of insect-proof screenhouse. *Acta Horticulturae* 1227: 205-212.

Teitel, M., Wenger, E., 2012. The effect of screenhouse roof shape on the flow patterns - CFD simulations. *Acta Horticulturae* 927: 604-610.

Valera, D.L., Molina, F.D., Álvarez, A.J., López, J.A., Terrés-Nicoli, J.M., Madueño, A. 2005. Contribution to characterisation of insect-proof screens: Experimental measurements in wind tunnel and CFD simulation. *Acta Horticulturae* 691: 441–448.

Vidogbéna, F., Adégbidi, A., Assogba-Komlan, F., Martin, T., Ngouajio, M., Simon, S., Parrot, L. 2015. Cost: benefit analysis of insect net use in cabbage in real farming conditions among smallholder farmers in Benin. *Crop Protection* 78: 164-171.

Villagrán, E., Bojacá, C., 2019b. CFD Simulation of the Increase of the Roof Ventilation Area in a Traditional Colombian Greenhouse: Effect on Air Flow Patterns and Thermal Behavior. *International Journal of Heat and Technology* 37: 881:892.

Villagrán, E.A., Romero, E.J.B., Bojacá, C.R. 2019. Transient CFD analysis of the natural ventilation of three types of greenhouses used for agricultural production in a tropical mountain climate. *Biosystems Engineering* 188: 288-304.

Villagrán, E.A., Bojacá, C.R., 2019a. Study of natural ventilation in a Gothic multi-tunnel greenhouse designed to produce rose (Rosa spp.) in the high-Andean tropic. *Ornamental Horticulture* 25: 133–143.

Wuepper, D., Wimmer, S., Sauer, J. 2020. Is small family farming more environmentally sustainable? Evidence from a spatial regression discontinuity design in Germany. *Land Use Policy* 90: 104360.

Xu, G., Liu, X., Wang, Q., Xiong, R., Hang, Y. 2017. Effects of screenhouse cultivation and organic materials incorporation on global warming potential in rice fields. *Environmental Science and Pollution Research* 24: 6581-6591.

Yang, G., Guo, Z., Ji, H., Sheng, J., Chen, L., Zhao, Y. 2018. Application of insect-proof nets in pesticide-free rice creates an altered microclimate and differential agronomic performance. *PeerJ* 6: 1-23.

Zorzeto, T.Q., Leal, P.A. M., Nunes, E.F., Araújo, H.F. 2014. Homogeneity of temperature and relative humidity of air in greenhouse. *International Proceedings of Chemical, Biological and Environmental Engineering* 79: 25-29.